Thermodynamic Analysis of a Designed Three-Stranded Coiled Coil

Judith A. Boice,[‡,§] Gregg R. Dieckmann,[||] William F. DeGrado,[||] and Robert Fairman*[,‡]

Bristol-Myers Squibb Pharmaceutical Research Institute, P.O. Box 4000, Princeton, New Jersey 08543-4000, and Johnson Research Foundation, Department of Biochemistry and Biophysics, University of Pennsylvania School of Medicine, Philadelphia, Pennsylvania 19104-6059

Received July 24, 1996[⊗]

ABSTRACT: The study and successful design of coiled-coil protein structural motifs have provided much insight into the rules governing protein folding and stability. In this work we use a thermodynamic approach to quantitate the rules that govern the specific oligomerization of coiled coils. We have designed a highly stable trimeric coiled coil by placing valine residues at each *a* position and leucine residues at each *d* position of the heptad repeating unit. The peptide forms a very stable trimer as determined by sedimentation equilibrium, and the concentration dependence of its circular dichroism spectrum follows a cooperative monomer/dimer/trimer equilibrium with the dimer state as a highly unstable intermediate. Its guanidinium chloride denaturation curve was collected at several peptide concentrations, and analysis of the data confirms the cooperativity of the trimerization process and provides a free energy of stabilization of −18.4 kcal mol^{-1} for the trimer. The heat capacity, ΔC_p, was measured by global analysis of thermal unfolding data collected at a number of guanidinium chloride concentrations. Guanidinium chloride induces cold denaturation in the thermal unfolding curves, providing a reasonably well-determined value for ΔC_p of 750 cal deg^{-1} mol^{-1}. This translates to a ΔC_p of 8.6 cal deg^{-1} mol^{-1} per residue and corresponds well to that expected of a coiled coil with a well-defined tertiary structure.

The α-helical coiled coil provides an excellent model system for investigating the forces that shape the structure of proteins. This structural motif has a geometric seven-residue repeat, which is generally reflected in the hydrophobicity of its amino acid sequence. A number of years ago, Hodges and co-workers prepared a series of polyheptapeptides with the sequence (Hb_a-Hp_b-Hp_c-Hb_d-Hp_e-Hp_f-$Hp_g)_n$, in which Hb and Hp are hydrophobic and hydrophilic amino acids and the subscripts refer to the position in the heptad repeat (Lau et al., 1984). These peptides self-assembled into highly helical oligomers, showing the importance of hydrophobic interactions in the assembly process (Figure 1a). More recently, the nature of the apolar amino acid residues at the *a* and *d* positions has been shown to have an important influence on the oligomerization state of GCN4-based coiled coils (Harbury et al., 1993). As the peptides associate, they seek to fully bury their hydrophobic residues while simultaneously adopting low-energy rotamers and optimizing their van der Waals interactions. The observed structures clearly reflect a compromise between optimizing these individual forces, as the crystal structure of a tetrameric coiled coil formed by a peptide with Leu at *a* and Ile at *d* contains a hole running down the central axis of the structure (Harbury et al., 1993). Breaks in the hydrophobic period can also have an important influence on the stoichiometry of the coiled coils. The presence of a single hydrophilic residue at *a* has been shown to favor the formation of dimers over other higher order structures, because the dimer has a relatively high solvent accessibility

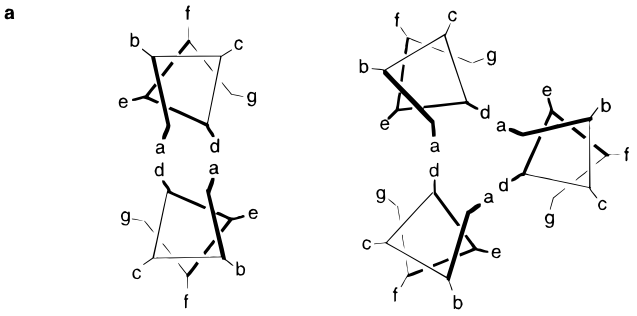

FIGURE 1: (a) Helical wheel diagram of two- and three-stranded coiled coils, showing the locations of the heptad positions in the structures. (b) Amino acid sequences of coil-Ser and coil-V_aL_d.

and hence does not require complete burial of the hydrophilic group (O'Shea et al., 1991, 1993; Betz et al., 1995).

Our own work has focused on a series of coiled coils modeled after one of Hodges' original design (O'Neil & DeGrado, 1990; Betz et al., 1995). It contains Leu residues at each *a* and *d* position and Glu and Lys at *e* and *g*, respectively. These charged residues can undergo favorable interhelical electrostatic interactions only if the structure is parallel in nature. Based on the early literature, it was assumed that these peptides would form parallel dimers, but a crystal structure of one member of this series of peptides, coil-Ser, showed an antiparallel trimeric structure (Lovejoy et al., 1993). The trimer appears to be favored over dimeric structures because it provided better dehydration of the hydrophobic side chains. As in the anticipated dimer, the trimer contains two helices docked in a parallel orientation with their apolar Leu residues associated in a hydrophobic interaction and salt bridges between Glu and Lys residues

* Author to whom correspondence should be addressed.
‡ Bristol-Myers Squibb Pharmaceutical Research Institute.
§ Present address: Department of Biochemistry, Merck Research Laboratories, Rahway, New Jersey 07065.
|| University of Pennsylvania School of Medicine.
⊗ Abstract published in *Advance ACS Abstracts,* November 1, 1996.

S0006-2960(96)01831-4 CCC: $12.00

at the helix−helix interface. However, a third helix docks in an antiparallel orientation against the parallel pair. Its Leu residues associate in layers with those from the other two helices forming an extensive hydrophobic core. The antiparallel orientation was unexpected because in this geometry the electrostatic interactions between this helix and its neighbors are potentially destabilizing and consist of one helix−helix interface that is rich in Lys residues, while the other interface is rich in Glu residues. While such an arrangement should be destabilizing at neutral pH, the peptide was crystallized at pH 5, near the pK_a of the Glu residues. At this pH some of the Glu residues are protonated and might form stabilizing hydrogen bonds with deprotonated Glu residues. In fact, two such hydrogen-bonded pairs, between residue Glu-A27 and Glu-C6, and Glu-A24 and Glu-A20 (numbering from the Protein Data Bank, entry 1COS), are apparent in the crystal structure based on the distance of their carboxylate oxygen atoms. Consistent with this interpretation, fluorescent derivatives of coil-Ser adopt parallel rather than antiparallel trimers in aqueous solution at neutral pH (Wendt et al., 1995).

A detailed study of the association of coil-Ser in aqueous solution showed that it exists in a noncooperative monomer/dimer/trimer equilibrium (Hill coefficient = 2.3), in which $\Delta G°$ for the formation of a dimer from two monomers was approximately equal to $\Delta G°$ for the formation of the trimer from a monomer and a dimer (Lovejoy et al., 1993). We therefore were interested in determining what changes could be made to the sequence of coil-Ser to provide it with a stronger preference for either a dimeric or trimeric oligomerization state. A single Asn or Ala residue at an *a* position is capable of favoring the dimeric oligomerization state (Betz et al., 1995), but less has been known concerning the features that might uniquely stabilize the trimeric state. In this paper, we demonstrate that a derivative of coil-Ser with Val at each *a* position (coil-V_aL_d) (Figure 1) cooperatively assembles into trimers.

EXPERIMENTAL PROCEDURES

Modeling. The coil-V_aL_d peptide was modeled as two- and three-helix coiled coils using the programs InsightII and Discover (Biosym). The method for generating coiled-coil structures from first principles has been described previously (Dieckmann, 1995; Betz & DeGrado, 1996). A dimeric model was also created beginning with the coordinates from the crystal structure of GCN4 (O'Shea et al., 1991). The side chains were replaced with those of coil-V_aL_d, utilizing the same side chain rotamers as found in the GCN4 structure.

Peptide Preparation. The coil-V_aL_d peptide was prepared using Fmoc-protected amino acids and techniques described previously (Choma et al., 1994). Peptide concentration was determined either by amino acid analysis (Liu & Boykins, 1989) or ninhydrin analysis (Rosen, 1957).

Sedimentation Equilibrium Ultracentrifugation. Experiments were performed using an An-60 Ti rotor in a Beckman Model XLA ultracentrifuge at 25 °C. The peptide loading concentration was 60 μM in 10 mM MOPS,[1] pH 7.5, and 150 mM NaCl. The NaCl is added to avoid charge density artifacts, and its addition has no appreciable effects on the stability or oligomeric state of the peptide. Data for the peptide were collected using six-channel Epon, charcoal-filled centerpieces with a 12 mm path length containing 110 μL samples and 125 μL buffer references. The samples were centrifuged at 25 000, 35 000, and 45 000 rpm, and the protein distribution was monitored at a wavelength of 242 nm. Ten successive radial scans were averaged using a 0.001 cm step size, and equilibrium was assumed if no change in distribution was observed over intervals of 2 h.

Data analysis software running under Igor (Wavemetrics, Lake Oswego, OR) and using the algorithm of Michael L. Johnson (Johnson et al., 1981) was a gift from Preston Hensley (Smith Kline Beecham, King of Prussia, PA). Data analysis was also done using the HID program from the Analytical Ultracentrifugation Facility at the University of Connecticut. The partial specific volume was calculated from the weight average of the partial specific volumes of the individual amino acids (Cohn & Edsall, 1943).

Circular Dichroism. Data were collected using an Aviv 62DS circular dichroism spectropolarimeter equipped with a thermoelectric device for temperature control. All measurements were made in 10 mM MOPS, pH 7.5, at 25 °C. Data for the GuHCl denaturation experiments were collected after sufficient time was allowed for the samples to reach equilibrium. Data for the thermal melts were collected at 222 nm using a 1° step, a bandwidth of 1.5 nm, an equilibration time of 2.5 min, and a data averaging time of 1 min. Thermal unfolding experiments were tested for thermodynamic equilibrium by requiring exact overlapping unfolding curves as a function of equilibration time.

Peptide concentration dependence data and GuHCl denaturation data were fit by nonlinear least-squares methods to various equilibrium schemes using a PC version of the program MLAB (Civilised Software, Bethesda, MD) (Knott, 1979). The formalism used in the curve fitting has been described previously (Fairman et al., 1995). Global fits using the thermal unfolding data were carried out as described below.

The following relationship describes a monomer/trimer equilibrium scheme:

$$[\theta]_{obs} = [\theta]_{mon}\frac{[monomer]}{[P_{tot}]} + [\theta]_{tri}\frac{3[monomer]^3}{K_3[P_{tot}]} \quad (1)$$

The variation of $[\theta]_{obs}$ on GuHCl concentration at constant temperature was treated using the following linear function (Santoro & Bolen, 1988) as described previously (Fairman et al., 1995) for a monomer/*n*-mer equilibrium:

$$[\theta]_{obs} = [\theta]_{mon}\frac{[monomer]}{[P_{tot}]} + [\theta]_n\frac{n[monomer]^n}{\exp\left(\frac{\Delta G^{H_2O} + m[GuHCl]}{-RT}\right)}\frac{1}{[P_{tot}]} \quad (2)$$

where ΔG^{H_2O} is the free energy of stability in the absence of GuHCl, *m* is the dependence of stability on GuHCl concentration (in units of kcal mol^{-1} M^{-1}), *T* is the temperature (in kelvin), *n* is the oligomerization state, and *R* is the universal gas constant. For experiments at variable temperature the term ΔG^{H_2O} is replaced by the Gibbs−Helmholtz function:

[1] Abbreviations: CD, circular dichroism; GuHCl, guanidinium chloride; SE, sedimentation equilibrium; MOPS, 3-morpholinopropanesulfonic acid.

$$\Delta G^{H_2O} = \Delta H^\circ - T\Delta S^\circ + \Delta C_p[T - T^\circ - T\ln(T/T^\circ)] \quad (3)$$

RESULTS AND DISCUSSION

Modeling. coil-V_aL_d was modeled as two- and three-stranded coiled coils to help to predict the structural features that might differentially stabilize these two association states. Because we were concerned with the association of the peptide at neutral pH, only parallel orientations were considered. At this pH, the Glu and Lys residues should be fully ionized, and repulsive electrostatic interactions should destabilize alternate antiparallel arrangements. The structures of the dimer and trimer were assembled from first principles using methods for the construction of coiled coils described previously (Dieckmann, 1995; Betz & DeGrado, 1996). This method requires the choice of a fixed rotamer for each interior residue. Val is known to adopt a single rotamer in α-helices ($\chi_1 = 165°$) (McGregor et al., 1987), and this value was used in all models (where χ_1 for Val is defined by atoms N, Cα, Cβ, and Cγ1). Leu can adopt two low-energy conformations in α-helices (McGregor et al., 1987), so two different models were generated for each oligomerization state: one in which all Leu residues have $\chi_1 = -175°$ and $\chi_2 = 75°$ (dimer$_t$) and a second model with $\chi_1 = -60°$ and $\chi_2 = -175°$ (dimer$_{g+}$) (for Leu, χ_1 is defined by N, Cα, Cβ, and Cγ and χ_2 by Cα, Cβ, Cγ, and Cδ1). To test the appropriateness of this modeling procedure, we also constructed a model of the dimer utilizing the backbone coordinates from the crystal structure of GCN4. The rmsd's between this model and the two dimeric coiled-coil models generated from first principles (Table 1) indicate that our modeling procedure generates structures with overall geometries that agree well with those observed in naturally occurring proteins.

As shown in Figure 2, efficient packing of the hydrophobic residues was observed in both the dimeric and trimeric oligomerization states. However, calculations based on the method of Eisenberg and McLachlan (Eisenberg & McLachlan, 1986; Eisenberg et al., 1989) suggest that hydration forces favor the formation of the trimer. The changes in solvation energy accompanying oligomerization are given in Table 1, computed for the two dimeric and trimeric models. On a per-monomer basis, the trimers consistently give more favorable solvation energies. In the models, efficient salt bridging is observed between Glu side chains at position *e* on one helix and Lys residues at position *g* of the preceding heptad on a neighboring helix in both the dimeric and trimeric structures.

Sedimentation Equilibrium. Sedimentation equilibrium ultracentrifugation indicates that coil-V_aL_d forms very stable trimers in aqueous solution (pH 7.5, 10 mM MOPS, 150 mM NaCl, 25 °C) as reported previously (Betz et al., 1995) and as shown in Figure 3. The peptide sediments as a single homogeneous species at concentrations between approximately 10 and 100 μM, indicating that it does not significantly change its association state within this concentration regime. Analysis of the data indicates that it sediments with an apparent molecular weight of 10 076 ± 210. This value is within 4% of that calculated for the trimer.

GuHCl-Induced Unfolding Curves. The thermodynamic stability of coil-V_aL_d was determined by monitoring its far-UV circular dichroism at 222 nm as a function of the concentration of GuHCl at a peptide concentration of 25 μM in 10 mM MOPS, pH 7.5 at 25 °C. The data are shown normalized to the fraction of trimer in Figure 4A. At low concentrations of GuHCl, the mean residue ellipticity at 222 nm ($[\theta]_{222}$) is approximately −36 000 deg cm^2/dmol, consistent with a fully helical conformation. At high concentrations of denaturant $[\theta]_{222}$ approaches zero, indicating that the monomer is largely unstructured. The denaturation curves are all sigmoidal with a single inflection point, consistent with a two-state equilibrium in which intermediates are minimally populated at equilibrium.

An interpretation of the GuHCl unfolding curves for associating peptides requires a knowledge of the cooperat-

Table 1: Comparison of Dimer and Trimer Models

model	χ_1 (Leu) (deg)	χ_2 (Leu) (deg)	rmsd (Å) (backbone)[a]	rmsd (Å) (heavy)[a,b]	ΔG°_s (kcal/mol per helix)[c]
dimer$_t$	−175	75	1.054	1.856	−15.8
dimer$_{g+}$[d]	−60	−175	0.930	1.764	−14.8
trimer$_t$	−175	75			−18.4
trimer$_{g+}$	−60	−175			−18.0

[a] Root mean square deviation between the model and the dimeric model generated from coordinates of GCN4. [b] All atoms except hydrogens. [c] Solvation free energies, $\Delta G^\circ_s = G_{s(folded)} - G_{s(unfolded)}$, were computed using the approach of Eisenberg (Eisenberg & McLachlan, 1986; Eisenberg et al., 1989) assuming an extended unfolded state. The values of ΔG°_s computed will depend on the choice of the unfolded state which defines $G_{s(unfolded)}$. However, this term cancels when the values of ΔG°_s are compared for two models ($\Delta\Delta G^\circ_s$) since the same unfolded state is used in calculating the ΔG°_s for each model. [d] Rotamer observed in the GCN4 structure.

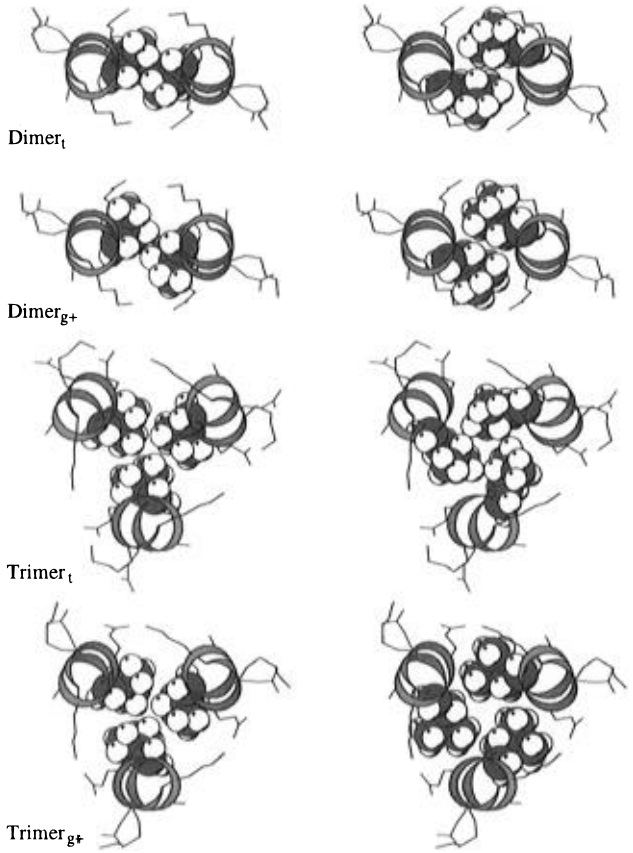

FIGURE 2: MOLSCRIPT (Kraulis, 1991) figure showing a slice through two- and three-stranded coiled-coil models of coil-V_aL_d illustrating the packing in hydrophobic layers. For each model, the Val residues in an *a* layer (left) and the Leu residues in a *d* layer (right) are shown as CPK surfaces.

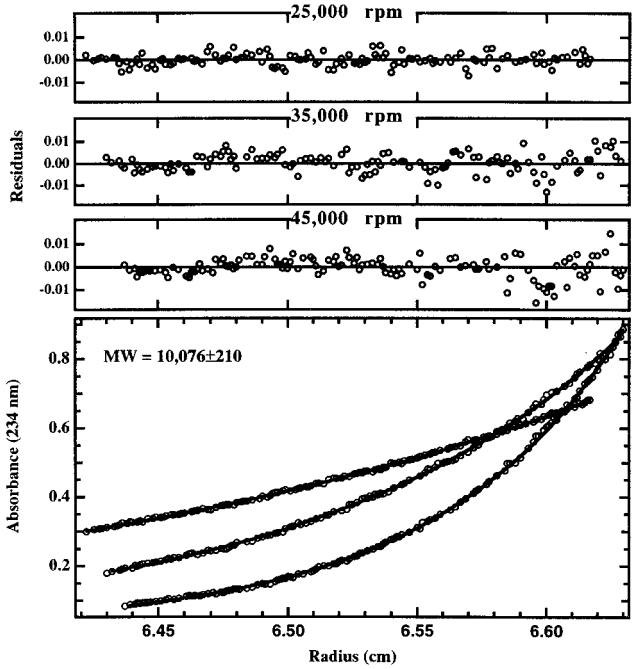

FIGURE 3: Sedimentation equilibrium analysis. Measurements were made using 60 μM coil-V_aL_d in 150 mM NaCl and 10 mM MOPS, pH 7.5, at 25 °C. Constants used for the data analysis are υ_{bar} = 0.761 mL/g; and ρ = 1.0017 g/mL. The data are shown fit to a single ideal species.

ivity of the association process. We therefore measured the peptide concentration dependence of $[\theta]_{222}$ near the midpoint of the GuHCl-induced unfolding transition (Figure 5). The isotherm is optimally fit with a Hill coefficient of 3.0 ± 0.2, indicating that the process shows a strong positive cooperativity (i.e., the formation of the dimer is the energetically difficult step in the assembly process). This finding contrasts with previous results for coil-Ser, which showed a Hill coefficient of 2.3 (Betz et al., 1995). The data were also fit to either a monomer/dimer or a cooperative monomer/trimer equilibrium. As expected from the observed Hill coefficient, the data were well described by the monomer/trimer but not by the monomer/dimer scheme.

To determine the free energies of dimerization and trimerization for coil-V_aL_d, the peptide concentration/ellipticity isotherm data were fit to a monomer/dimer/trimer equilibrium in which [P] is the concentration of coil-V_aL_d, and K_2 and K_3 are the dissociation constants for the dimer $(P)_2$ and trimer $(P)_3$:

$$(P)_3 \overset{K_3}{\rightleftharpoons} 1.5(P)_2 \overset{K_2}{\rightleftharpoons} 3P$$

$$K_3 = [P][(P)_2]/[(P)_3] \qquad K_2 = [P]^2/[(P)_2]$$

The overall free energy of association, $RT\ \ln(K_2K_3)$ is extremely well determined by the data, but because of the high degree of cooperativity of the curve and the covariance of K_2 and K_3, the values of the individual equilibrium constants are less well determined. The best fit to the data gave values of $K_2 = 5 \times 10^{-4}$ M and $K_3 = 2 \times 10^{-6}$ M. However, the value of K_2 can be varied 2−3-fold without significantly affecting the quality of the fit as long as K_3 was allowed to compensate in an opposite direction. On the basis of this observation, it appears that the ratio of K_2 to K_3 is at least 50, although it may be much larger. By

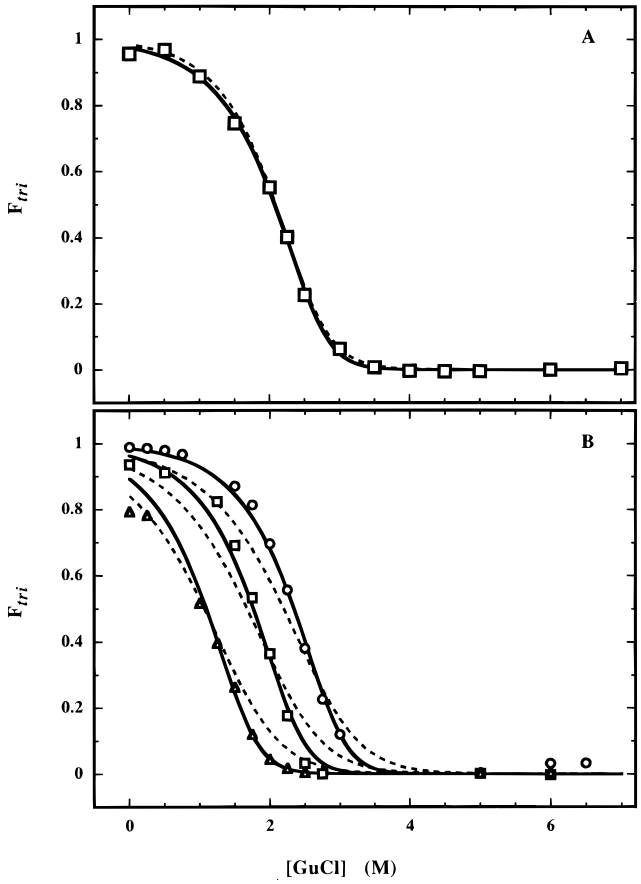

FIGURE 4: GuHCl dependence. (A) Measurements were made using 25 μM coil-V_aL_d in 10 mM MOPS, pH 7.5, at 25 °C. The data are shown fit to monomer/trimer (—) and monomer/dimer (- - -) models using a linear function for [GuHCl] dependence and a linear function for the unfolded baseline. The curve-fitting parameters and their associated errors for the monomer/trimer model are as follows: $K_3 = 3.2 \pm 1.4 \times 10^{-14}$ M^2 [$\Delta G_{H_2O} = -18\,400$ cal mol^{-1}; $\Delta G_{2\ M\ GuHCl} = -12\,900$ cal mol^{-1}]; $m_{[GuHCl]} = -2740 \pm 160$ cal mol^{-1} M^{-1}; $\theta_{max} = -36\,600 \pm 500$ deg cm^2 dmol^{-1}; $\theta_{min} = -2690 \pm 840$ deg cm^2 dmol^{-1}; monomer slope = -420 ± 160 deg cm^2 dmol^{-1} M^{-1}. (B) Measurements were made using 5, 25, and 100 μM coil-V_aL_d. All three data sets were fit simultaneously to either monomer/trimer (—) or monomer/dimer (- - -) equilibrium schemes.

contrast, the ratio of K_2 to K_3 for coil-Ser is near unity. Figure 5B shows that the data for coil-V_aL_d are not well fit when the ratio of K_2 to K_3 is forced to be 1.0 in the fitting algorithm.

Having established the cooperativity and stoichiometry of the association process, the entire GuHCl-induced denaturation curve (Figure 4) was evaluated to determine the free energy of trimerization of coil-V_aL_d in the absence of denaturant. This analysis involved making the usual assumptions that the transition was two state (in this case unfolded monomers going to α-helical trimers) and that the free energy of folding scaled linearly with [GuHCl] (Santoro & Bolen, 1988). The free energy of trimerization extrapolated to 0 M GuHCl was -18.4 ± 0.2 kcal mol^{-1}. This free energy corresponds to a transition midpoint of 0.31 μM for the association of the peptide to form trimers in the absence of denaturant.

For comparison, the data were also fit with a monomer/dimer equilibrium scheme. Note that if only one denaturation curve collected at one peptide concentration is analyzed, this method is insensitive to the final oligomer state as the data are equally well fit by either a monomer/dimer and monomer/

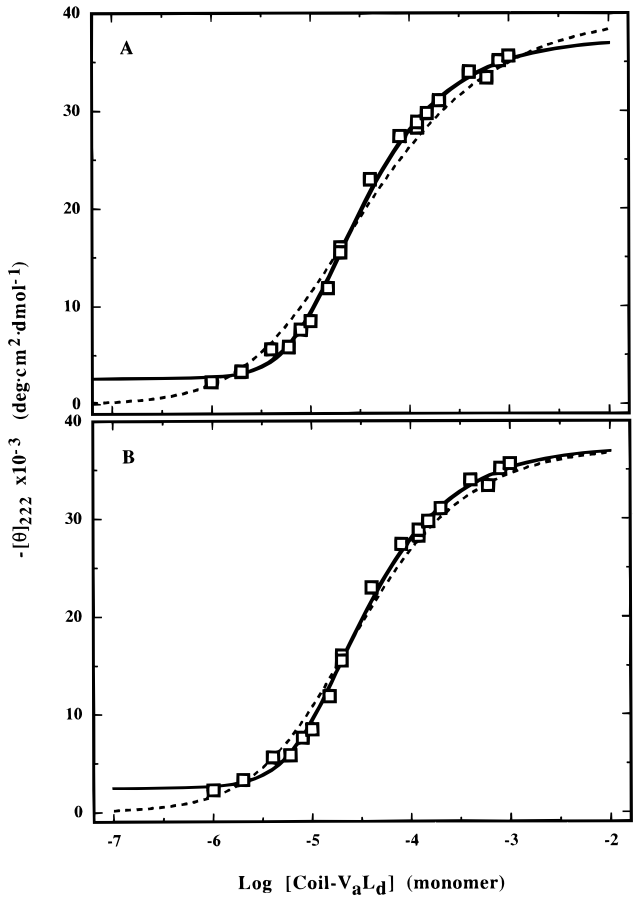

FIGURE 5: Peptide concentration dependence. (A) Data shown were fit with either monomer/trimer (—) or monomer/dimer (- - -) models. (B) Data were fit with independent K_2 and K_3 (—) or with $K_2 = K_3$ (- - -). Measurements were made in 2 M GuHCl and 10 mM MOPS, pH 7.5, at 25 °C. The curve-fitting parameters and their associated errors are as follows: mon/dim: $K_2 = 3.6 \pm 0.92 \times 10^{-5}$ M [$(M_T)_{1/2}$ = 36 μM]; $\theta_{max} = -40\,000 \pm 1300$ deg cm^2 dmol^{-1}; $\theta_{min} = 0 \pm 1600$ deg cm^2 dmol^{-1}. mon/tri: $K_3 = 8.2 \pm 0.94 \times 10^{-10}$ M^2 [$(M_T)_{1/2}$ = 33 μM; $\Delta G_{2\ M\ GuHCl} = -12\,400$ cal mol^{-1}]; $\theta_{max} = -37\,400 \pm 400$ deg cm^2 dmol^{-1}; $\theta_{min} = -2600 \pm 400$ deg cm^2 dmol^{-1}. mon/dim/tri: $K_2 = 4.8 \pm 11 \times 10^{-4}$ M; $K_3 = 1.8 \pm 4.8 \times 10^{-6}$ M; $\theta_{max} = -37\,600 \pm 500$ deg cm^2 dmol^{-1}; $\theta_{min} = -2300 \pm 900$ deg cm^2 dmol^{-1}.

trimer treatment. However, the quality of the fits becomes sensitive to the association scheme if the GuHCl-induced unfolding curves are collected at several different peptide concentrations (Figure 4) and fit globally using the method described in Experimental Procedures. Clearly, a monomer/trimer equilibrium scheme provides a better fit than that for a monomer/dimer scheme. If the degree of oligomerization is treated as an adjustable parameter in the global fit, a value of 3.18 ± 0.25 is obtained for the *n*-mer state.

Thermal Unfolding. The thermal denaturation of proteins provides information concerning the nature and cooperativity of the interactions stabilizing their structures. Molten globule proteins tend to have rather diffuse thermal unfolding curves, with low values of ΔC_p and $\Delta H°$, while native proteins have cooperative unfolding transitions with a larger ΔC_p and $\Delta H°$. coil-V$_a$L$_d$ shows a cooperative thermal unfolding ($\Delta H° = -39.2 \pm 0.2$ kcal mol^{-1} at 25 °C) transition in the absence of GuHCl. To determine ΔC_p for the transition, the unfolding curves were repeated in the presence of increasing concentrations of GuHCl (Figure 6), which decreases the observed enthalpy of the transition but has been observed

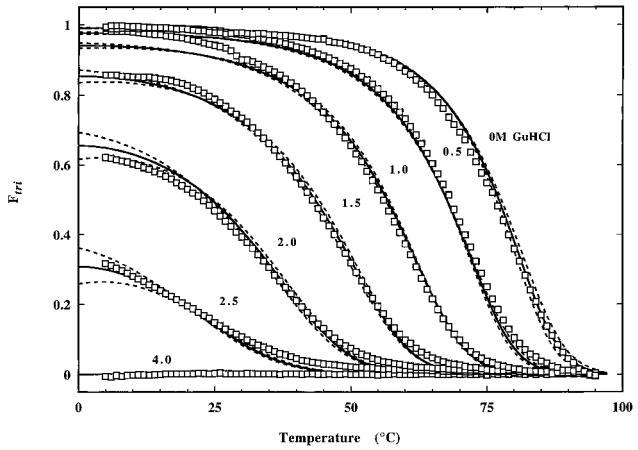

FIGURE 6: Thermal unfolding. Measurements were made using 33 μM coil-V$_a$L$_d$ in 10 mM MOPS, pH 7.5. Solid lines represent the global best fit using the equations described in Experimental Procedures. Dashed lines represent fits to the data where ΔC_p was fixed using values of ±100 cal deg^{-1} mol^{-1} from the best fit value. Baselines were fit using only the 0 and 4 M GuHCl data for native and unfolded baselines, respectively. Parameter values from fits to determine baselines: $[\theta]_{monomer} = -330 \pm 140$ deg cm^2 dmol^{-1} (at 273 K); $[\theta]_{monomer}$ slope = -27.22 ± 0.41 deg cm^2 dmol^{-1} deg^{-1}; $[\theta]_{trimer} = -33\,870 \pm 480$ deg cm^2 dmol^{-1} (at 273 K); $[\theta]_{trimer}$ slope = 128.2 ± 1.9 deg cm^2 dmol^{-1} deg^{-1}. Parameter values from global fits to 0, 0.5, 1.0, 1.5, 2.0, 2.5, and 4.0 M GuHCl data using 25 °C as the reference temperature: $m_{[GuHCl]} = -3407 \pm 17$ cal mol^{-1} M^{-1}; $\Delta H° = 39\,250 \pm 210$ cal mol^{-1}; $\Delta S° = 20\,080 \pm 180$ cal mol^{-1}; $\Delta C_p = 752.9 \pm 8.9$ cal deg^{-1} mol^{-1} (8.6 cal deg^{-1} mol^{-1} per residue).

to have a rather minor effect on ΔC_p (Makhatadze & Privalov, 1992). The apparent decrease in the plateau for the folded signal can be explained simply by the convergence of cold- and heat-denaturation thermal transitions and is an important effect for obtaining well-determined values for ΔC_p and ΔH. The thermal unfolding curves were fit globally using the Gibbs−Helmholtz equation as described in Experimental Procedures. The free energy evaluated at 25 °C ($\Delta G = -18.8$ kcal mol^{-1}) agrees well with that determined by the GuHCl denaturation method described above (−18.4 kcal mol^{-1}). The computed value of ΔC_p for the transition is 750 cal deg^{-1} mol^{-1}, and a sensitivity analysis indicated that this value was accurate to within approximately 100 cal deg^{-1} mol^{-1}. Small, but nonrandom deviations in the quality of the fits probably reflect variations in ΔC_p with both temperature (Hagihara et al., 1994) and [GuHCl] (Makhatadze & Privalov, 1992). Expressed on a per residue basis, the change in the heat capacity difference between the folded and unfolded states amounts to 8.6 cal deg^{-1} mol^{-1}.

Surprisingly, values of ΔC_p have been measured for only a few associating peptide systems, and these values vary greatly. Values of ΔC_p range from as high as 20.7 cal deg^{-1} mol^{-1} per residue for the VBP dimeric coiled coil (measured by analysis of CD thermal unfolding curves) (Krylov et al., 1994) to as low as 3.8 cal deg^{-1} mol^{-1} per residue for the GCN4 dimeric coiled coil (measured calorimetrically) (Thompson et al., 1993). Our work on the tetrameric coiled coil from Lac repressor, Lac21 (Fairman et al., 1995), gave an intermediate value of 14.8 cal deg^{-1} mol^{-1} per residue (Fairman, unpublished results). We have also measured a value of 8.8 cal deg^{-1} mol^{-1} per residue for a designed tetrameric coiled-coil peptide that shows native-like properties in solution (Betz & DeGrado, 1996). Probably the most careful thermodynamic analysis has been reported for melittin

(Wilcox & Eisenberg, 1992; Hagihara et al., 1994). Wilcox and Eisenberg (1992) reported a range of values of ΔC_p of 9.3−13.2 cal deg^{-1} mol^{-1} per residue. This result was confirmed and more rigorously tested by Goto and colleagues (1994), who compared the values of ΔC_p obtained from van't Hoff and calorimetric analyses. They found that ΔC_p for melittin has a significant temperature dependence, particularly at high temperatures, but otherwise behaved as a two-state system since the two methods gave good agreement.

CONCLUSIONS

The current challenge in protein design is choosing a primary sequence that will define a specific tertiary structure. The greatest progress in defining rules for tertiary structure has been in the design of coiled-coil protein folds, particularly in defining specific oligomerization states. We have been interested in gaining a thermodynamic understanding of these rules. Toward this aim, we have designed a highly cooperative all-parallel trimeric coiled coil, coil-V_aL_d, containing valine at *a* positions and leucine at *d* positions of each heptad repeat and have measured its thermodynamic parameters.

First, we show that the folding of coil-V_aL_d is highly cooperative as measured by following the acquisition of secondary structure as a function of peptide concentration. In contrast to GCN4-pVL (Harbury et al., 1993), a coiled coil also containing the motif V_aL_d, and coil-Ser (Betz et al., 1995), the dimeric state is a highly unstable intermediate in the monomer/trimer equilibrium. The trimer state is very stable, exhibiting a free energy of −18.4 kcal mol^{-1} as measured by global fits to [GuHCl] dependence of stability measured at several peptide concentrations.

To test the nature of the tertiary structure, we measured the thermal unfolding of the coil-V_aL_d peptide as a function of GuHCl concentration. Under these conditions we see both cold and heat denaturation as evidenced by the suppression of the signal at the low-temperature plateau in the data. These data were fit globally to the Gibbs−Helmholtz equation, assuming a two-state folding function, resulting in a ΔC_p of 8.6 cal deg^{-1} mol^{-1} per residue. This value is somewhat smaller than that observed for globular proteins with well-defined tertiary structures but well within the range of values of ΔC_p that have been observed for coiled coils. The wide range reported in the literature does not appear to correlate to any biophysical characteristic of this class of protein fold and merits further study.

ACKNOWLEDGMENT

We thank Clifford Klimas for amino acid analysis, John Desjarlais for use of his program for the calculation of solvent-accessible surface areas, and Jim Lear for implementing the use of MLAB and for helpful discussions.

REFERENCES

Betz, S. F., & DeGrado, W. F. (1996) *Biochemistry 35*, 6955−6962.

Betz, S., Fairman, R., O'Neil, K., Lear, J., & DeGrado, W. (1995) *Philos. Trans. R. Soc. London B 348*, 81−88.

Choma, C. T., Lear, J. D., Nelson, M. J., Dutton, P. L., Robertson, D. E., & DeGrado, W. F. (1994) *J. Am. Chem. Soc. 116*, 856−865.

Cohn, E. J., & Edsall J. T. (1943) in *Proteins, Amino Acids and Peptides as Ions and Dipolar Ions*, pp 370−381, Reinhold Publishing Corp., New York.

Dieckmann, G. R. (1995) Dissertation, University of Michigan.

Eisenberg, D., & McLachlan, A. D. (1986) *Nature 319*, 199−203.

Eisenberg, D., Wesson, M., & Yamashita, M. (1989) *Chem. Scr. 29A*, 217−221.

Fairman, R., Chao, H.-G., Mueller, L., Lavoie, T. B., Shen, L., Novotny, J., & Matsueda, G. R. (1995) *Protein Sci. 4*, 1457−1469.

Hagihara, Y., Oobatake, M., & Goto, Y. (1994) *Protein Sci. 3*, 1418−1429.

Harbury, P. B., Zhang, T., Kim, P. S., & Alber, T. (1993) *Science 262*, 1401−1407.

Johnson, M. L., Correia, J. J., Yphantis, D. A., & Halverson, H. R. (1981) *Biophys. J. 36*, 575−588.

Knott, G. D. (1979) *Comput. Programs Biomed. 10*, 271−280.

Kraulis, P. J. (1991) *J. Appl. Crystallogr. 24*, 946−950.

Krylov, D., Mikhailenko, I., & Vinson, C. (1994) *EMBO J. 13*, 2849−2861.

Lau, S. Y. M., Taneja, A. K., & Hodges, R. S. (1984) *J. Biol. Chem. 259*, 13253−13261.

Liu, T. Y., & Boykins, R. A. (1989) *Anal. Biochem. 182*, 383−387.

Lovejoy, B., Choe, S., Cascio, D., McRorie, D. K., DeGrado, W. F., & Eisenberg, D. (1993) *Science 259*, 1288−1293.

Makhatadze, G. I., & Privalov, P. L. (1992) *J. Mol. Biol. 226*, 491−505.

McGregor, M. J., Islam, S. A., & Sternberg, M. J. (1987) *J. Mol. Biol. 198*, 295−310.

O'Neil, K. T., & DeGrado, W. F. (1990) *Science 250*, 646−651.

O'Shea, E. K., Klemm, J. D., Kim, P. S., & Alber, T. A. (1991) *Science 254*, 539−544.

O'Shea, E. K., Lumb, K. J., & Kim, P. S. (1993) *Curr. Biol. 3*, 658−667.

Rosen, H. (1957) *Arch. Biochem. Biophys. 67*, 10−15.

Santoro, M. M., & Bolen D. W. (1988) *Biochemistry 27*, 8063−8067.

Thompson, K. S., Vinson C. R., & Freire E. (1993) *Biochemistry 32*, 5491−5496.

Wendt, H., Berger, C., Baici, A., Thomas, R. M., & Bosshard, H. R. (1995) *Biochemistry 34*, 4097−4107.

Wilcox, W., & Eisenberg, D. (1992) *Protein Sci. 1*, 641−653.

BI961831D